J. Fluid Mech. (1979), *vol.* 95, *part* 3, *pp.* 497–513
Printed in Great Britain

Steady flow between a rotating circular cylinder and fixed square cylinder

By E. LEWIS

Department of Mathematics, University of Bristol, England

(Received 17 November 1978)

Numerical solutions have been obtained for the problem of steady, incompressible, viscous flow between two infinite concentric cylinders, the cross-sections of the inner and outer cylinders being circular and square respectively. The square cylinder is fixed and the flow is driven by the rotation of the circular cylinder. Solutions are given for Reynolds number in the range 1–1400 and for several values of the parameter B, defined as the ratio of the side of the square to the diameter of the circle.

1. Introduction

Numerical techniques have been applied to many problems involving the solution of the incompressible Navier–Stokes equations but relatively few of these problems have involved flow in a closed region. The most notable exceptions are that of flow in a closed rectangular cavity (Kawaguti 1961; Burggraf 1966; Greenspan 1969, 1973) and that of flow between two concentric circular cylinders of finite length (Meyer 1969; Rogers & Beard 1969).

The present problem considers the flow between two infinite concentric cylinders, the outer one being square with side $2b$ and the inner being circular of radius a. The flow is driven by the rotation of the circular cylinder and by varying the parameter $B = b/a$ it is possible to generate very large eddies in the corners. One can also show the existence of a sequence of eddies dying away into the corner as described theoretically by Moffatt (1964) and illustrated numerically by Pan & Acrivos (1967) and Collins & Dennis (1976).

An interesting feature of the problem is the difficulty posed by the incompatibility of the boundaries, in that a uniform finite difference mesh in either Cartesian or polar co-ordinates does not allow all boundary grid points to lie on the intersection of grid lines. This problem is circumvented by using a non-uniform mesh so that boundary points are also grid points. This mesh complicates the finite difference equations considerably if second-order approximations for the derivatives are used, but this difficulty is overcome by first of all solving first-order finite difference approximations for the Navier–Stokes equations and then incorporating difference corrections to bring the accuracy up to second order.

There is, too, the further complication of having to determine the correct value of the stream function on the circular boundary, assuming that the stream function on the square boundary is zero. This difficulty arises due to the multiple connectedness of the flow region. Any constant value of the stream function on the circular boundary

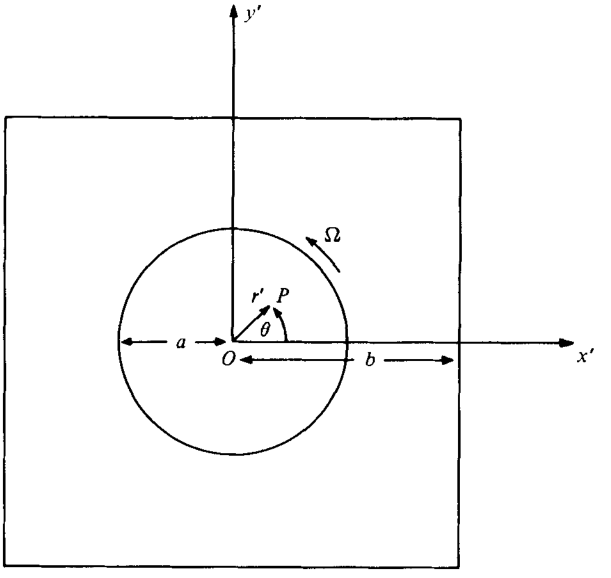

FIGURE 1. The co-ordinate system.

specifies a solution but the particular value needed is that which makes the pressure between the cylinders single-valued.

The numerical procedure used is reasonably standard and similar to that used by such authors as Burggraf (1966), Greenspan (1969), Collins & Dennis (1975, 1976).

2. The equations of motion

Because of the geometry of the problem it is convenient to use both Cartesian and polar co-ordinates. A cross-section of the cylinders is shown in figure 1, where the common centre O is taken as the origin. The co-ordinates of any point P of the cross-section are given by (x', y') or (r', θ) where primes denote that the variables are dimensional. If the velocity components at P are (u', v') then a stream function ψ' and vorticity ζ' can be defined by

$$u' = \partial\psi'/\partial y', \quad v' = -\partial\psi'/\partial x', \quad \zeta' = \partial u'/\partial y' - \partial v'/\partial x'.$$

This definition of the vorticity is the negative of the usual definition, namely the curl of the velocity vector. In terms of the radius a and angular velocity Ω of the circular cylinder, dimensionless variables are defined by

$$x' = ax, \quad y' = ay, \quad r' = ar,$$
$$u' = a\Omega u, \quad v' = a\Omega v,$$
$$\psi' = a^2\Omega\psi, \quad \zeta' = \Omega\zeta,$$

so that the steady-state incompressible Navier–Stokes equations become

$$\frac{\partial^2\psi}{\partial x^2} + \frac{\partial^2\psi}{\partial y^2} = \zeta, \tag{1a}$$

$$\frac{\partial^2\zeta}{\partial x^2} + \frac{\partial^2\zeta}{\partial y^2} = -R\left(\frac{\partial\psi}{\partial x}\frac{\partial\zeta}{\partial y} - \frac{\partial\psi}{\partial y}\frac{\partial\zeta}{\partial x}\right), \tag{1b}$$

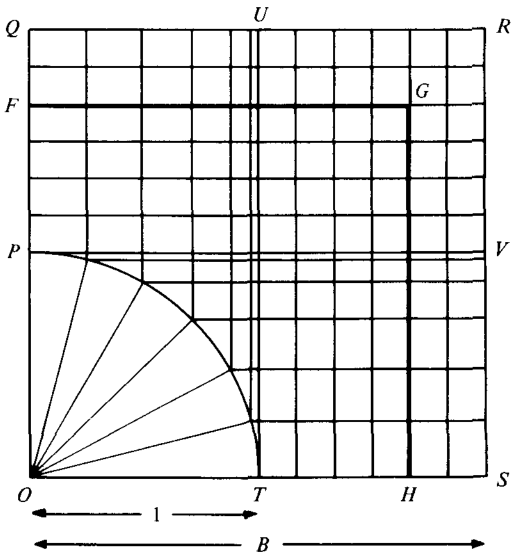

FIGURE 2. Finite difference grid for the case $n = 6$, $l = 6$.

where R is the Reynolds number $a^2\Omega/\nu$, ν being the coefficient of kinematic viscosity.

The circular cylinder is given by $r = 1$ while the sides of the square are given by $x = \pm B$, $y = \pm B$, where B is the non-dimensional parameter b/a. There are, therefore, two parameters for the problem: R representing the balance of viscous and inertia forces and B representing the geometry.

The boundary conditions are

$$\psi = \frac{\partial\psi}{\partial x} = \frac{\partial\psi}{\partial y} = 0 \quad \text{on the sides} \quad x = \pm B, \quad y = \pm B, \tag{2a}$$

$$\psi = \psi_c, \quad \text{a constant}, \quad \frac{\partial\psi}{\partial x} = -x, \quad \frac{\partial\psi}{\partial y} = -y \quad \text{on} \quad r = 1. \tag{2b}$$

The value of ψ_c cannot be specified in advance and has to be determined as part of the problem. It is fixed by imposing the condition that the pressure be single-valued in the region between the two cylinders.

Since the flow is periodic, period $\frac{1}{2}\pi$, with respect to the angle θ, consideration of the flow region is confined to the first quadrant. Boundary conditions are therefore required on $x = 0$ and $y = 0$ and these are taken to be the usual periodic boundary conditions

$$\psi(\lambda, 0) = \psi(0, \lambda), \quad \zeta(\lambda, 0) = \zeta(0, \lambda),$$

$$\frac{\partial\psi}{\partial y}(\lambda, 0) = -\frac{\partial\psi}{\partial x}(0, \lambda) \quad \text{and} \quad \frac{\partial\zeta}{\partial y}(\lambda, 0) = -\frac{\partial\zeta}{\partial x}(0, \lambda) \tag{3}$$

for all λ such that $1 \leqslant \lambda \leqslant B$.

3. Finite difference equations

The region $PQRST$ under consideration is covered by a rectangular grid as shown in figure 2. This grid is obtained by first of all dividing the arc PT into n equal intervals.

The grid points so formed on PT are then taken to define the mesh lines parallel to the x axis for the region $PVST$ and those parallel to the y axis for the region $PQUT$. The remainder of the mesh is formed by dividing the intervals PQ and TS into l equal intervals of width h where $lh = B-1$. This finite difference scheme has the disadvantage of being non-uniform but has the attraction of making all grid points on the boundary lie at the intersection of mesh lines.

If (x, y) is a typical grid point and h_1, h_2, h_3, h_4 are the mesh lengths adjacent to (x, y) then, in the usual notation, the points (x, y), $(x+h_1, y)$, $(x, y+h_2)$, $(x-h_3, y)$, $(x, y-h_4)$ are denoted by $0, 1, 2, 3, 4$.

Using central difference approximations, equation $(1a)$ is approximated by

$$A_0\psi_0 - A_1\psi_1 - A_2\psi_2 - A_3\psi_3 - A_4\psi_4 = -\zeta_0 h_2 h_4 + C_0, \tag{4}$$

where

$$A_0 = \frac{2h_2h_4}{h_1h_3} + 2, \quad A_1 = \frac{2h_2h_4}{h_1(h_1+h_3)}, \quad A_2 = \frac{2h_4}{h_2+h_4}, \quad A_3 = \frac{2h_2h_4}{h_3(h_1+h_3)}, \quad A_4 = \frac{2h_2}{h_2+h_4}$$

and

$$C_0 = -h_2h_4\frac{(h_1-h_3)}{3}\left(\frac{\partial^3\psi}{\partial x^3}\right)_0 - h_2h_4\frac{(h_2-h_4)}{3}\left(\frac{\partial^3\psi}{\partial y^3}\right)_0.$$

If C_0 is neglected the finite difference approximation (4) to $(1a)$ is only first order while if C_0 is included the approximation is second order. C_0 is called the difference correction and its use is described in §4.

To obtain the finite difference equation corresponding to $(1b)$, $(\partial\psi/\partial x)_0$ and $(\partial\psi/\partial y)_0$ are first of all approximated by

$$\alpha = \left(\frac{\partial\psi}{\partial x}\right)_0 = \frac{h_3^2\psi_1 + (h_1^2-h_3^2)\psi_0 - h_1^2\psi_3}{h_1h_3(h_1+h_3)},$$

$$\beta = \left(\frac{\partial\psi}{\partial y}\right)_0 = \frac{h_4^2\psi_2 + (h_2^2-h_4^2)\psi_0 - h_2^2\psi_4}{h_2h_4(h_2+h_4)}.$$

Then, using the technique of forward and backward differences (Greenspan 1969) or, as it is frequently referred to, upwind differencing (Roache 1976), the finite difference equation for the vorticity is

$$B_0\zeta_0 - B_1\zeta_1 - B_2\zeta_2 - B_3\zeta_3 - B_4\zeta_4 = D_0, \tag{5}$$

where the coefficients B_i are

$$B_2 = \frac{2h_4}{h_2+h_4} + R\alpha h_4, \quad B_4 = \frac{2h_2}{h_2+h_4}, \quad \alpha \geqslant 0;$$

$$B_2 = \frac{2h_4}{h_2+h_4}, \quad B_4 = \frac{2h_2}{h_2+h_4} - R\alpha h_4, \quad \alpha < 0;$$

$$B_1 = \frac{2h_2h_4}{h_1(h_1+h_3)}, \quad B_3 = \frac{2h_2h_4}{h_3(h_1+h_3)} + R\frac{\beta h_2h_4}{h_3}, \quad \beta \geqslant 0;$$

$$B_1 = \frac{2h_2h_4}{h_1(h_1+h_3)} - R\frac{\beta h_2h_4}{h_3}, \quad B_3 = \frac{2h_2h_4}{h_3(h_1+h_3)}, \quad \beta < 0;$$

$$B_0 = \frac{2h_2h_4}{h_1h_3} + 2 + R|\alpha|h_4 + R|\beta|\frac{h_2h_4}{h_3}, \quad \text{all } \alpha, \beta;$$

and the difference correction D_0 is defined as

$$D_0 = \frac{Rh_2h_4}{2}\left[\alpha H\left(\frac{\partial^2\zeta}{\partial y^2}\right)_0 + \beta H^*\left(\frac{\partial^2\zeta}{\partial x^2}\right)_0\right] - h_2h_4\frac{(h_1-h_3)}{3}\left(\frac{\partial^3\zeta}{\partial x^3}\right)_0 - h_2h_4\frac{(h_2-h_4)}{3}\left(\frac{\partial^3\zeta}{\partial y^3}\right)_0,$$

where

$$H = -h_2 \quad \text{if} \quad \alpha \geqslant 0, \qquad H^* = -h_3 \quad \text{if} \quad \beta \geqslant 0,$$

$$H = h_4 \quad \text{if} \quad \alpha < 0, \qquad H^* = h_1 \quad \text{if} \quad \beta < 0.$$

The boundary conditions for (4) are

$$\psi = 0 \quad \text{on } QR \text{ and } RS,$$

$$\psi = \psi_c \quad \text{on } PT, \tag{6}$$

periodic conditions on PQ and TS.

To obtain the boundary conditions for the vorticity equation (5) consider first the boundary RS. If (x, y) is a point on this boundary then ψ_3 can be obtained as a Taylor series expansion about this point, namely

$$\psi_3 = \psi_0 - h_3\left(\frac{\partial\psi}{\partial x}\right)_0 + \frac{h_3^2}{2}\left(\frac{\partial^2\psi}{\partial x^2}\right)_0 + O(h_3^3).$$

Now

$$\psi_0 = \left(\frac{\partial\psi}{\partial x}\right)_0 = 0$$

by ($2a$) and

$$\left(\frac{\partial^2\psi}{\partial x^2}\right)_0 = -\left(\frac{\partial v}{\partial x}\right)_0.$$

But

$$\zeta_0 = \left(\frac{\partial u}{\partial y}\right)_0 - \left(\frac{\partial v}{\partial x}\right)_0 = -\left(\frac{\partial v}{\partial x}\right)_0$$

since u is constant along the wall RS. Therefore

$$\psi_3 = \frac{h_3^2}{2}\zeta_0 + O(h_3^3),$$

giving

$$\zeta_0 = \frac{2\psi_3}{h_3^2} + O(h_3)$$

$$= \frac{2\psi_3}{h^2} + O(h)$$

because $h_3 = h$ for points (x, y) on RS.

The boundary conditions for ζ on QR and PT can be obtained in a similar manner although on PT expansions are required in both the x and y directions (for ψ_1 and ψ_2) which are subsequently added together to obtain $(\partial^2\psi/\partial x^2)_0 + (\partial^2\psi/\partial y^2)_0$ which is then replaced by ζ_0.

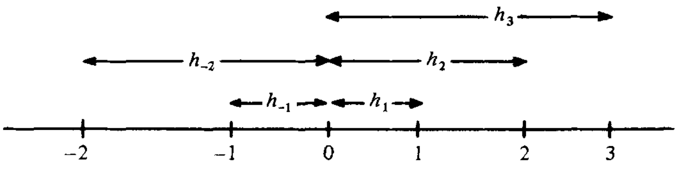

FIGURE 3. Mesh lengths for calculating difference correction at point O.

Therefore the boundary conditions for (5) can be expressed as

$$\zeta_0 = \frac{2\psi_3}{h^2} \quad \text{on } RS,$$

$$\zeta_0 = \frac{2\psi_4}{h^2} \quad \text{on } QR, \tag{7}$$

$$\zeta_0 = \frac{2}{h_1^2}(\psi_1-\psi_c)+\frac{2}{h_2^2}(\psi_2-\psi_c)+\frac{2x_0}{h_1}+\frac{2y_0}{h_2} \quad \text{on } PT,$$

periodic conditions on PQ and TS.

These boundary conditions have leading-error terms which are first order in the mesh lengths while equations (4) and (5) are second order provided the difference corrections are included. However, experience with using higher-order expressions to calculate the boundary vorticity has generally shown no significant improvement in the results and has often indicated convergence problems (Roache 1976) so it was decided not to experiment with higher-order formulae. Such formulae would also have been extremely cumbersome for the boundary $r = 1$.

Difference corrections

With reference to figure 2, the set of all interior grid points plus those grid points on PQ, but excluding P and Q, is denoted by S_h. The set of grid points on the boundaries PT and QRS is denoted by R_h. The derivatives comprising the difference corrections C_0 and D_0 in equations (4) and (5) respectively are calculated by the method of undetermined coefficients (Isaacson & Keller 1966). If (x, y) is the point at which the corrections are to be determined, let it and its neighbours in the x direction be numbered as in figure 3. Then at all points of S_h the approximation for $\partial^2\zeta/\partial x^2$ is

$$\left(\frac{\partial^2\zeta}{\partial x^2}\right)_0 \sim \gamma_{-1}\zeta_{-1}+\gamma_0\zeta_0+\gamma_1\zeta_1,$$

where $$\gamma_{-1} = \frac{2}{h_1(h_1+h_{-1})}, \quad \gamma_1 = \frac{2}{h_{-1}(h_1+h_{-1})}, \quad \gamma_0 = -(\gamma_1+\gamma_{-1}).$$

For all points of $S_h \cap PQUT$, but excluding those points which are one mesh length in the x direction from the boundary PT, the approximation for $\partial^3\zeta/\partial x^3$ is

$$\left(\frac{\partial^3\zeta}{\partial x^3}\right)_0 \sim \gamma_{-2}\zeta_{-2}+\gamma_{-1}\zeta_{-1}+\gamma_0\zeta_0+\gamma_1\zeta_1+\gamma_2\zeta_2,$$

where

$$\gamma_{-2} = \frac{6(h_{-1}-h_1-h_2)}{h_{-2}(h_{-2}-h_{-1})(h_{-2}+h_1)(h_{-2}+h_2)}, \quad \gamma_{-1} = \frac{6(h_{-2}-h_1-h_2)}{h_{-1}(h_{-1}-h_{-2})(h_{-1}+h_1)(h_{-1}+h_2)},$$

$$\gamma_1 = \frac{6(h_{-2}+h_{-1}-h_2)}{h_1(h_1-h_2)(h_1+h_{-1})(h_1+h_{-2})}, \quad \gamma_2 = \frac{6(h_{-2}+h_{-1}-h_1)}{h_2(h_2-h_1)(h_2+h_{-1})(h_2+h_{-2})},$$

$$\gamma_0 = -(\gamma_{-1}+\gamma_{-2}+\gamma_1+\gamma_2);$$

while for points of S_h which are adjacent to PT the approximation is

$$(\partial^3\zeta/\partial x^3)_0 \sim \gamma_{-1}\zeta_{-1}+\gamma_0\zeta_0+\gamma_1\zeta_1+\gamma_2\zeta_2+\gamma_3\zeta_3,$$

where

$$\gamma_{-1} = \frac{-6(h_1+h_2+h_3)}{h_{-1}(h_{-1}+h_3)(h_2+h_{-1})(h_1+h_{-1})}, \quad \gamma_1 = \frac{6(h_2+h_3-h_{-1})}{h_1(h_1-h_3)(h_2-h_1)(h_1+h_{-1})},$$

$$\gamma_2 = \frac{6(h_{-1}-h_1-h_3)}{h_2(h_2-h_3)(h_2+h_{-1})(h_2-h_1)}, \quad \gamma_3 = \frac{6(h_{-1}-h_1-h_2)}{h_3(h_3-h_2)(h_3+h_{-1})(h_3-h_1)},$$

$$\gamma_0 = -(\gamma_{-1}+\gamma_1+\gamma_2+\gamma_3).$$

No approximation for $\partial^3\zeta/\partial x^3$ is necessary in the region $URST$ since the mesh length in the x direction is uniform in this region.

Similar approximations hold for the derivatives with respect to y where the region $PVST$ now takes the place of the region $PQUT$.

4. The numerical procedure

The numerical procedure is obtained by an iterative procedure consisting of steps 1–6 described below. This sequence of steps corresponds to the procedure for a given choice of ψ_c. The method by which ψ_c is chosen is described in § 5.

Step 1. Set $k = 0$. Set initial values for $\psi^{(0)}, \zeta^{(0)}$ at all points of S_h (S_h and R_h are as defined in § 3). Set $\psi^{(0)} = \psi_c$ on PT and $\psi^{(0)} = 0$ on QRS. Set the difference corrections C_0 and D_0 to zero at all points of S_h. Set CORRECTION = FALSE.

Step 2. Solve equation (4) for $\psi^{(k+1)}$ on S_h with $\zeta = \zeta^{(k)}$ using the method of successive over-relaxation (SOR) with relaxation parameter ω_ψ. The iteration is continued until the maximum difference between respective values of ψ on successive iterations is less than ϵ_ψ or the number of iterations is greater than 10.

Step 3. Calculate the value $\zeta_b^{(k+1)}$ at all points of R_h using (7) with the recently calculated $\psi^{(k+1)}$ for ψ. Determine $\zeta^{(k+1)}$ on the boundary using the smoothing formula

$$\zeta^{(k+1)} = \gamma\zeta^{(k)} + (1-\gamma)\zeta_b^{(k+1)},$$

where γ is a positive constant < 1.

Step 4. Solve equation (5) for $\zeta^{(k+1)}$ on S_h using SOR with relaxation parameter ω_ζ. The convergence criterion is the same as that given in step 2 with ϵ_ζ taking the role of ϵ_ψ.

Step 5. Determine $\max|\psi^{(k+1)}-\psi^{(k)}|$, $\max|\zeta^{(k+1)}-\zeta^{(k)}|$ over all points of $S_h \cup R_h$ and if these quantities are not less than $\delta_\psi, \delta_\zeta$ respectively then set $k = k+1$ and go to step 2. Otherwise, if CORRECTION is FALSE set $k = k+1$ and go to step 6 else stop.

Step 6. Using the value of ψ and ζ just obtained calculate the difference corrections C_0 and D_0 on S_h. Set CORRECTION = TRUE and go to step 2.

5. Results

Results have been obtained for $B = 1{\cdot}05$, $1{\cdot}1$ and $2{\cdot}0$ with R ranging from 1 to 500, 1 to 1000 and 1 to 1400 respectively. The grid is determined by n and l as defined in § 3. For $B = 2$ and $R = 1$, 200, 500, 700 grids defined by $n = 10$, $l = 20$; $n = l = 20$ and $n = 20$, $l = 40$ were tried. The results were compared by examining the maximum

Grid	R			
	1	200	500	700
$n = 10, l = 20$	0·4665	0·4527	0·4400	0·4325
$n = 20, l = 20$	0·4655	0·4520	0·4405	0·4355
$n = 20, l = 40$	0·4656	0·4539	0·4465	0·4423

TABLE 1. Maximum values of ψ for varying grid sizes.

Grid	R			
	1	200	500	700
$n = 10, l = 20$	1·0206	1·2487	1·3088	1·3142
$n = 20, l = 20$	1·0171	1·2467	1·3080	1·3294
$n = 20, l = 40$	1·0186	1·2559	1·3430	1·3693

TABLE 2. Maximum values of ζ for varying grid sizes.

values of ψ and ζ and these are given in tables 1 and 2 respectively. These tables indicate that the results are qualitatively correct with the maximum stream function and maximum vorticity varying by at most 3 % and 4 % respectively, the differences being largest for $R = 700$. Subsequently all results were obtained with $n = 20$, $l = 40$ for $B = 2$ and $n = 40$, $l = 20$ for $B = 1{\cdot}05$ and $1{\cdot}1$.

Various values of the SOR parameters $\omega_\psi, \omega_\zeta$ were tried and it was found that $\omega_\psi = 1{\cdot}8$, $\omega_\zeta = 1{\cdot}2$ worked successfully in all cases. The parameters $\epsilon_\psi, \epsilon_\zeta, \delta_\psi, \delta_\zeta$ were all taken to be 10^{-4}, this being considered sufficient for the qualitative results being sought. The smoothness factor γ was taken to be 0·95 for the coarser grids but it was found necessary to take $\gamma = 0{\cdot}98$ for the 20/40 and 40/20 grids.

For each value of B a trial value of ψ_c was obtained by considering the exact solution for the analogous problem of flow between concentric circular cylinders of radii 1 and B (Batchelor 1967). For this problem the stream function on the inner cylinder is given by

$$\psi = -\frac{1}{2}+\frac{B^2}{B^2-1}\ln B.$$

This value of ψ was always too small but was near enough the correct value to provide a good initial guess which guaranteed convergence for $R = 1$. Solutions were then obtained for neighbouring values of ψ_c and for each of these solutions the pressure difference $\Delta P(r)$ between corresponding points on PQ and TS was calculated by integration of $\partial p/\partial x$ and $\partial p/\partial y$ along lines parallel to the x and y directions respectively as represented typically by the pair of lines FG and GH shown in figure 2. The required value of ψ_c was that for which $\Delta P(r) \equiv 0$ but in practice this was impossible to achieve since $\Delta P(r)$ oscillated about zero. Instead the accepted value of ψ_c was that for which $\max|\Delta P(r)|$ was minimized and it was possible to determine this value of ψ_c quite quickly since it was found that $\Delta P(r)$ varied almost linearly with ψ_c. Table 3 gives the values of ψ_c for $B = 1{\cdot}05$, $1{\cdot}1$ and $2{\cdot}0$ and R in the range 1 to 1400.

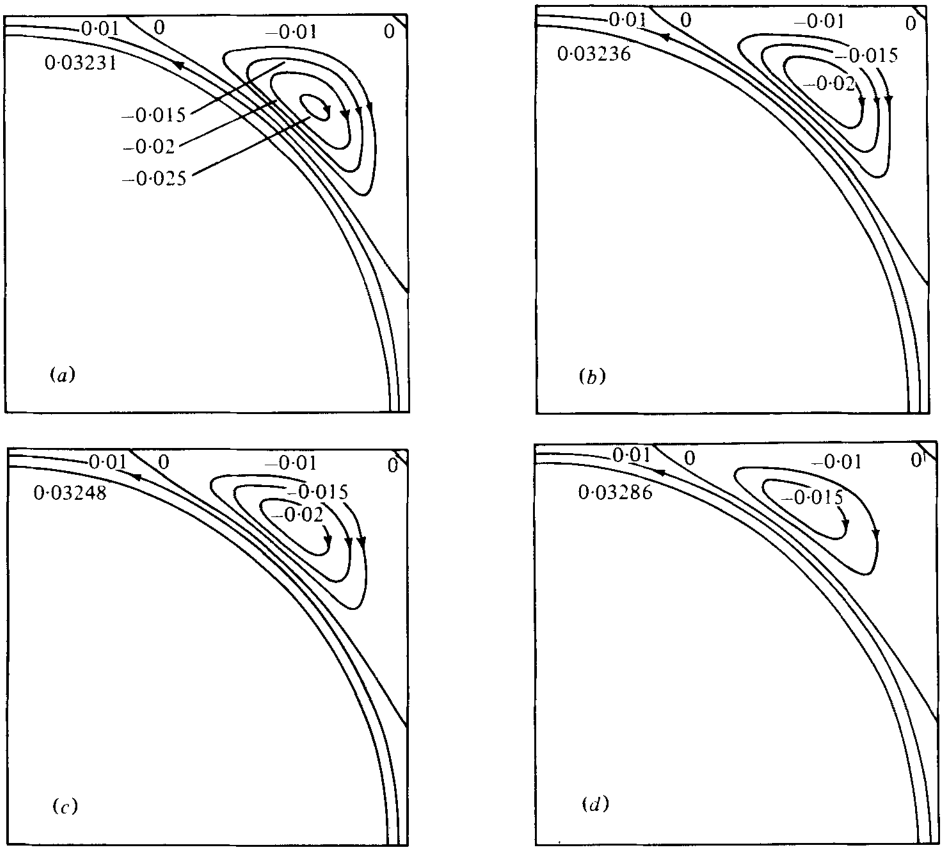

FIGURE 4. Streamlines ψ = constant for $B = 1{\cdot}05$ and (a) $R = 1$, (b) $R = 100$, (c) $R = 200$, (d) $R = 500$.

	B		
R	1·05	1·1	2·0
1	0·03231	0·06257	0·4656
100	0·03236	0·06264	0·4577
200	0·03248	0·06270	0·4539
500	0·03286	0·06212	0·4465
1000	—	0·06005	0·4375
1400	—	—	0·4314

TABLE 3. Values of the stream function on the circular cylinder $r = 1$.

Graphs for the streamlines and lines of constant vorticity for $B = 1{\cdot}05$ and $R = 1$, 100, 200, 500 are given in figures 4 and 5; those for $B = 1{\cdot}1$ and $R = 1$, 100, 200, 500, 1000 in figures 6 and 7; and those for $B = 2{\cdot}0$ and $R = 1$, 100, 200, 500, 1000, 1400 in figures 8 and 9. Since the flow is the same in each quadrant the streamlines and vorticity curves are shown only for the first quadrant except in the case $B = 2{\cdot}0$, $R = 200$ when the whole region is shown so that the swirl effect of the vorticity curves can be better appreciated. The solutions for fixed B and increasing R were obtained using the solution for some lower value of R as the initial guess. This procedure enabled

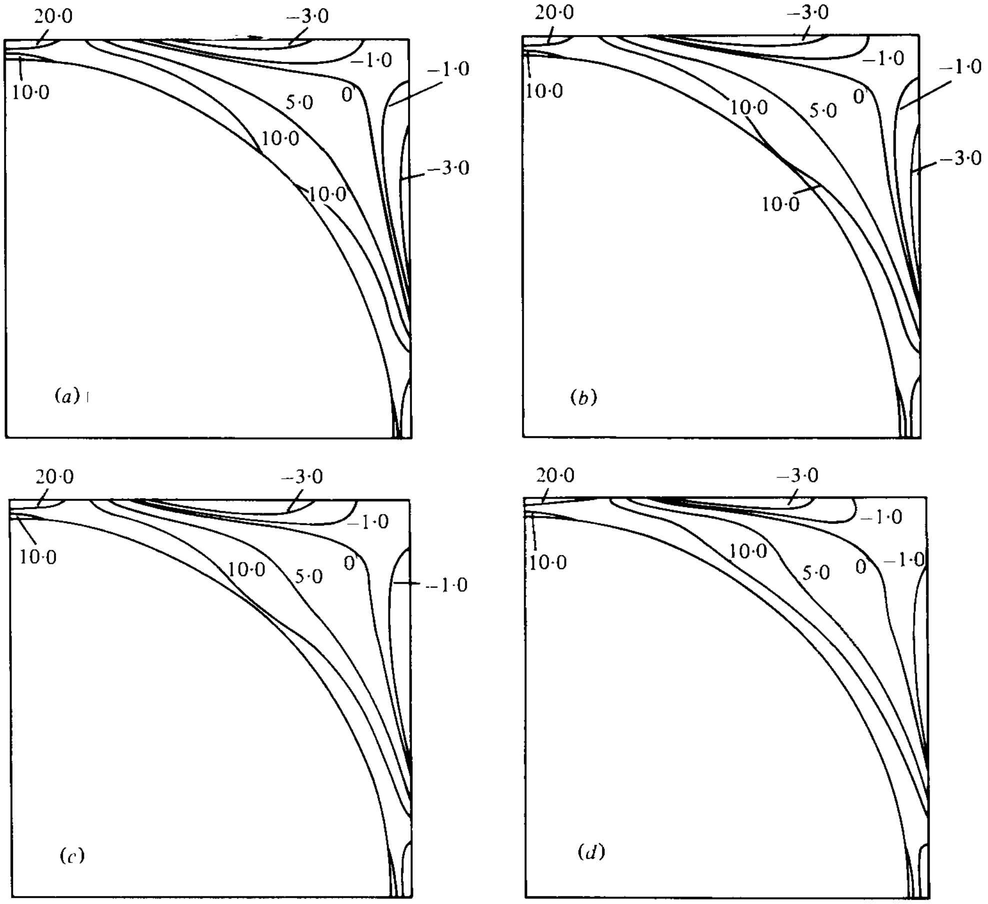

FIGURE 5. Curves of constant vorticity for $B = 1{\cdot}05$ and (a) $R = 1$, (b) $R = 100$, (c) $R = 200$, (d) $R = 500$.

solutions to be obtained as far as $R = 1400$ in the case of $B = 2$ but it became necessary to proceed in smaller and smaller increments of R as R increased. In the case of $B = 1{\cdot}1$ and $1{\cdot}05$ it required excessively small increments in R to proceed further than $R = 1000$ and $R = 500$ respectively and consequently no results have been obtained for higher values of R in these cases.

For $B = 2$ there is little change in the distribution of ψ between the cylinder $r = 1$ and the streamline $\psi = 0{\cdot}1$ as R increases although, for $R = 1400$, ψ_c is about 7 % less than its value for $R = 1$. The primary eddy in the corner, however, grows considerably and its intensity, measured as the maximum absolute value of ψ, increases from $0{\cdot}00014$ for $R = 1$ to $0{\cdot}00271$ for $R = 500$ varying only slightly thereafter as R increases to 1400 (see figure 10).

The curves of constant vorticity for $B = 2{\cdot}0$ are symmetric at $R = 1$ but then become pulled around in the direction of rotation as R increases, forming 'tongues' of vorticity protruding into the fluid. This swirl effect is particularly noticeable for $R = 200$. As R increases further these 'tongues' of vorticity become confined in a narrower and narrower band enclosing the circular cylinder whilst outside this band a region of flow develops for which the vorticity curves are almost circles centred on the origin.

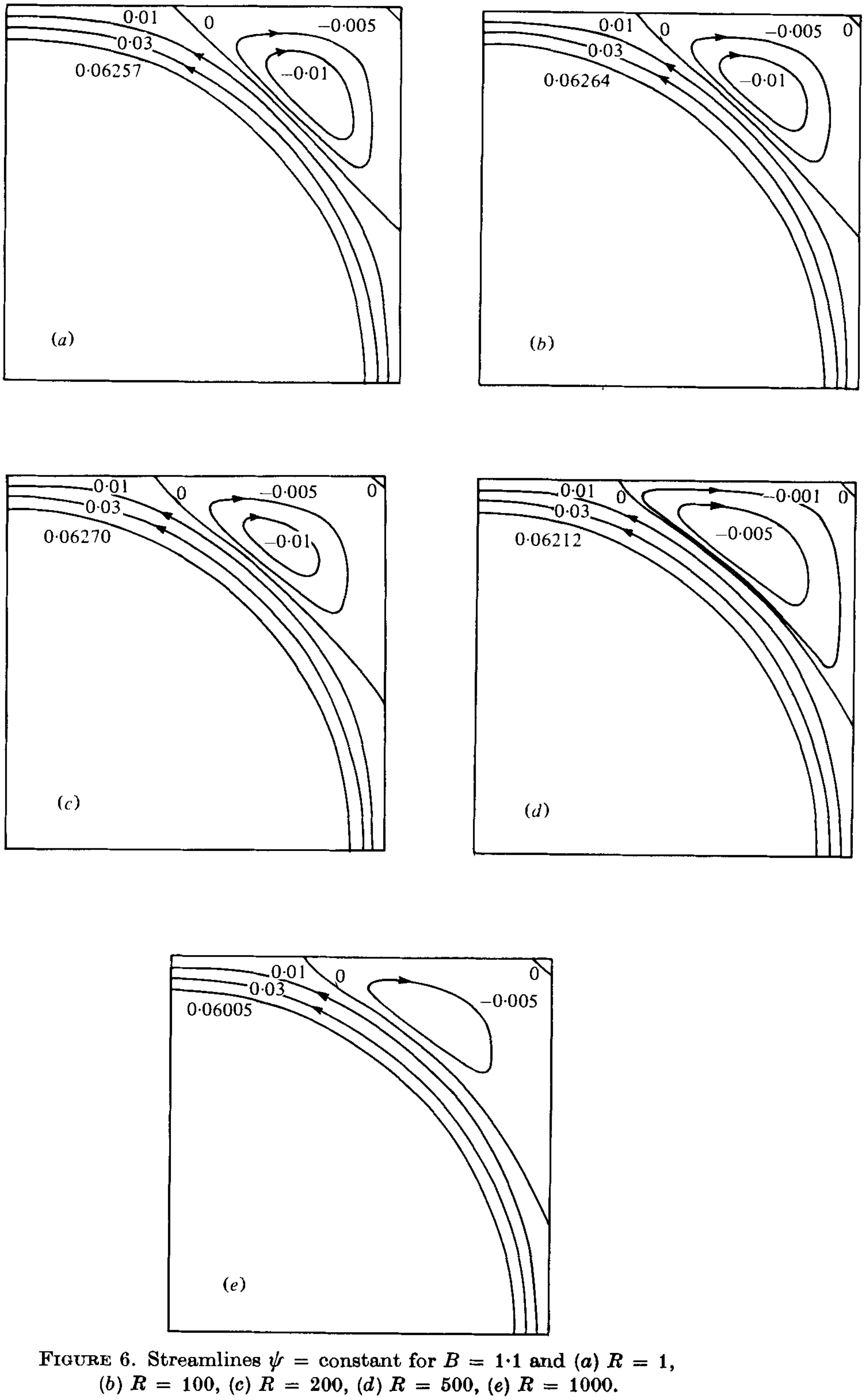

FIGURE 6. Streamlines ψ = constant for $B = 1{\cdot}1$ and (*a*) $R = 1$, (*b*) $R = 100$, (*c*) $R = 200$, (*d*) $R = 500$, (*e*) $R = 1000$.

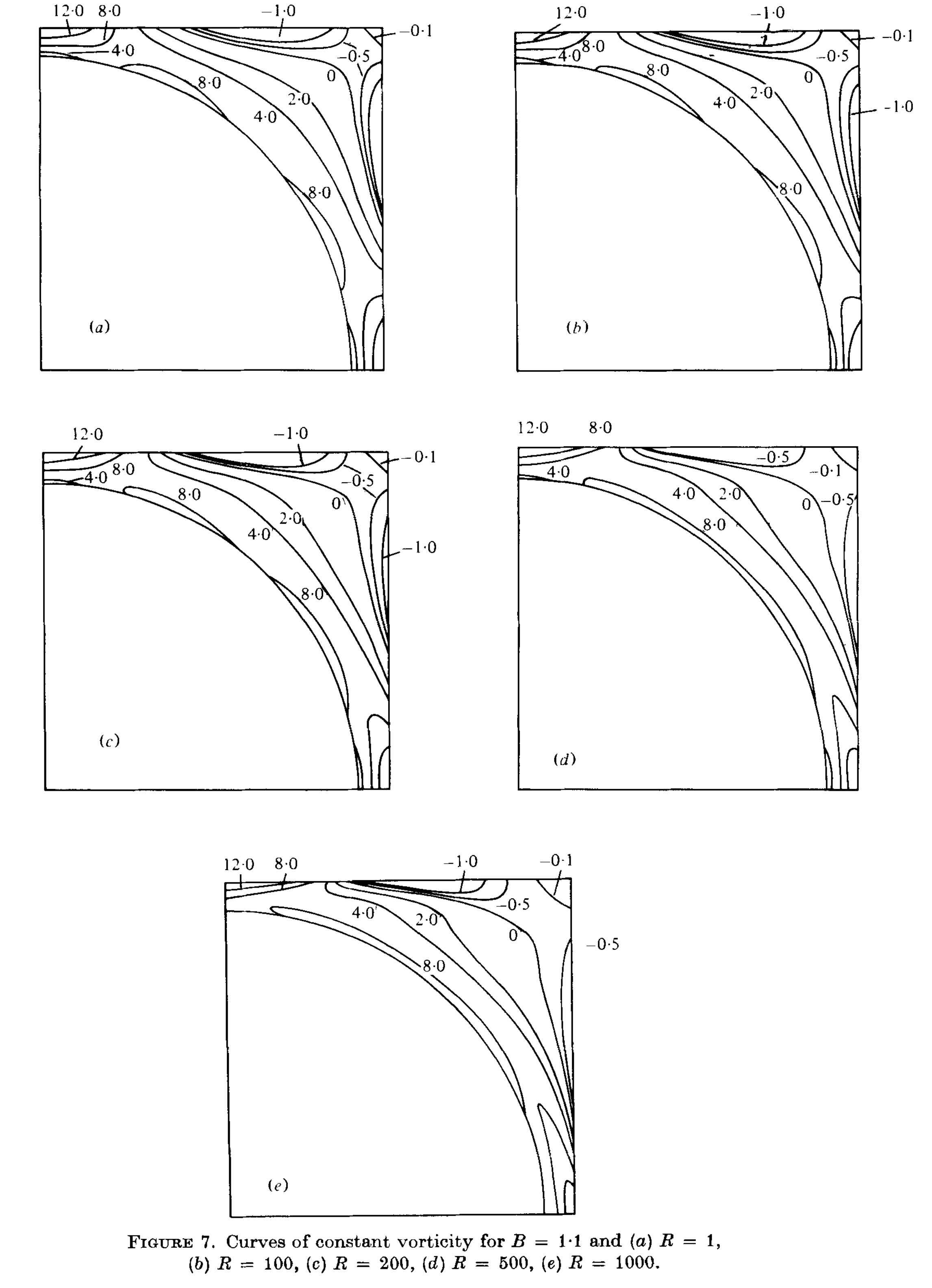

FIGURE 7. Curves of constant vorticity for $B = 1{\cdot}1$ and (*a*) $R = 1$, (*b*) $R = 100$, (*c*) $R = 200$, (*d*) $R = 500$, (*e*) $R = 1000$.

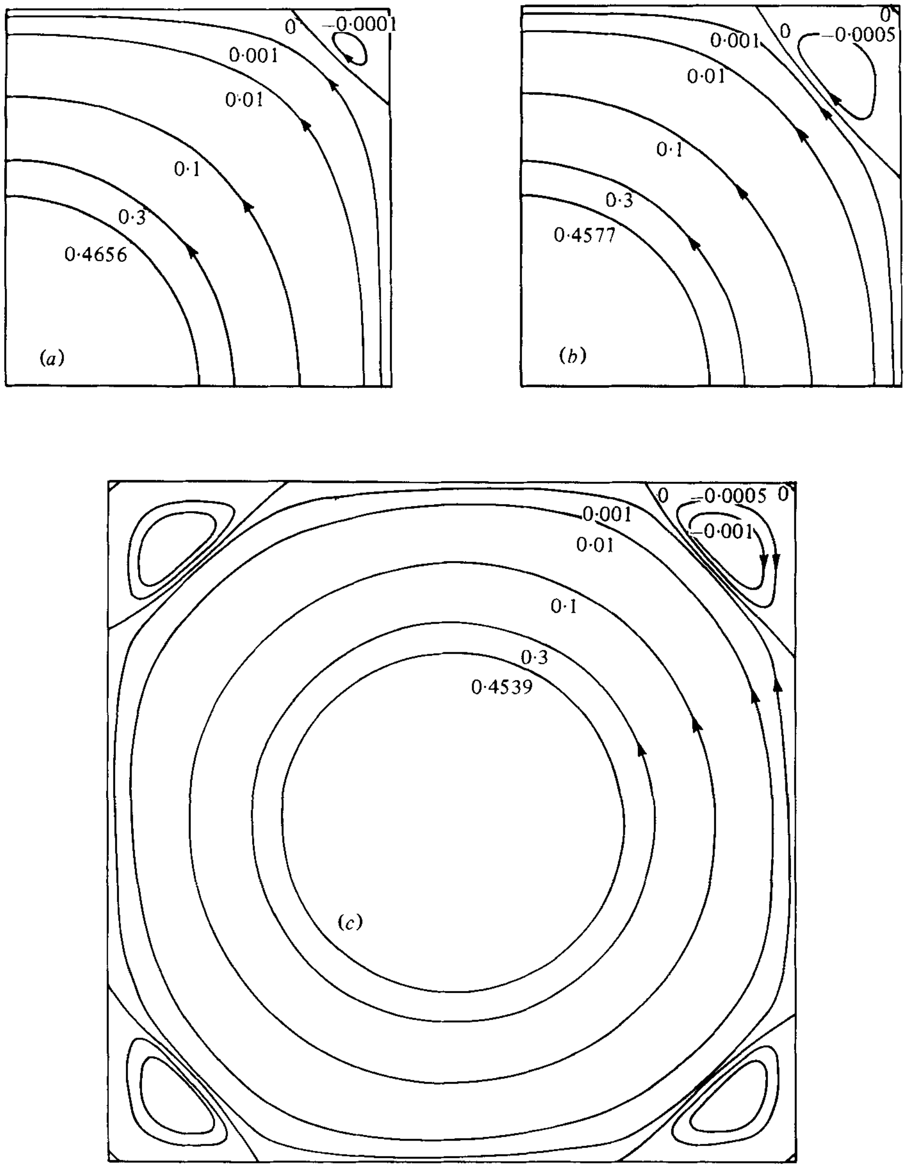

FIGURE 8 (a), (b), (c). For legend see p. 510.

In this region the flow behaves very much like that for flow between concentric circular cylinders. In fact in this latter case, for cylinders of radii $r = 1$ and $r = 2$, the vorticity is everywhere constant and of value 2/3 whilst for the present problem with $R = 1400$ there is clearly a large region with vorticity between 0·6 and 0·7. The occurrence of a large region of fluid between the cylinders for which the vorticity is approximately constant is in accordance with the theory of Batchelor (1956).

The results for $B = 1{\cdot}05$ and $B = 1{\cdot}1$ are similar to each other. In each case there is little change in the streamlines or the size of the primary corner eddy as R increases although the *shape* of the separating streamline changes, particularly near the points

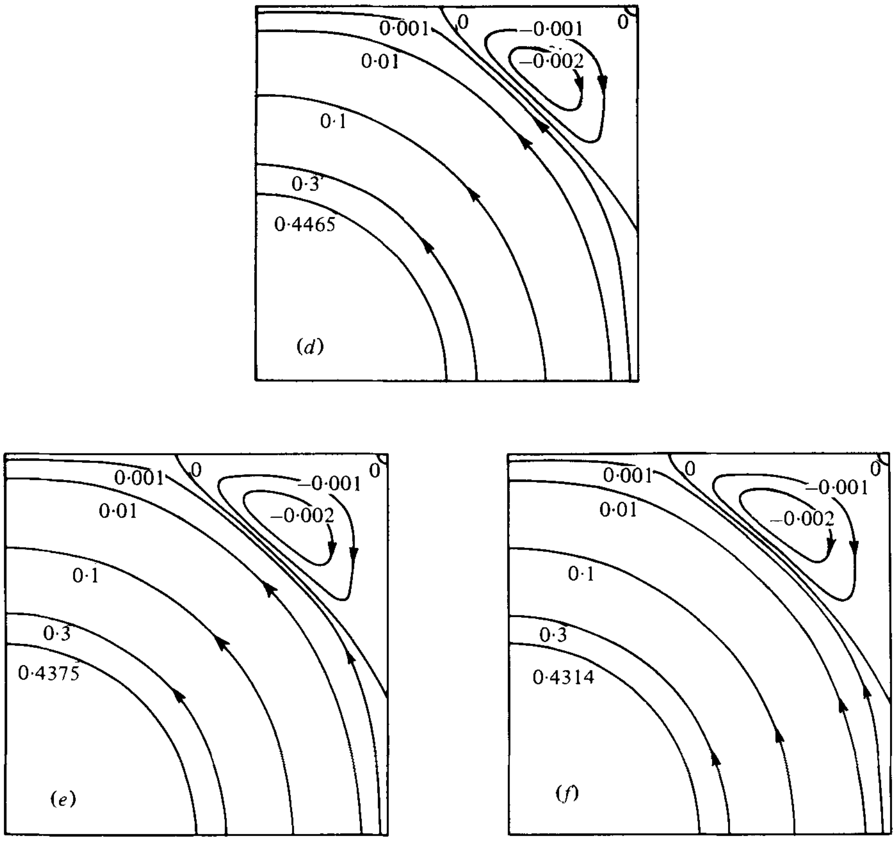

FIGURE 8. Streamlines ψ = constant for $B = 2{\cdot}0$ and (a) $R = 1$, (b) $R = 100$, (c) $R = 200$, (d) $R = 500$, (e) $R = 1000$, (f) $R = 1400$.

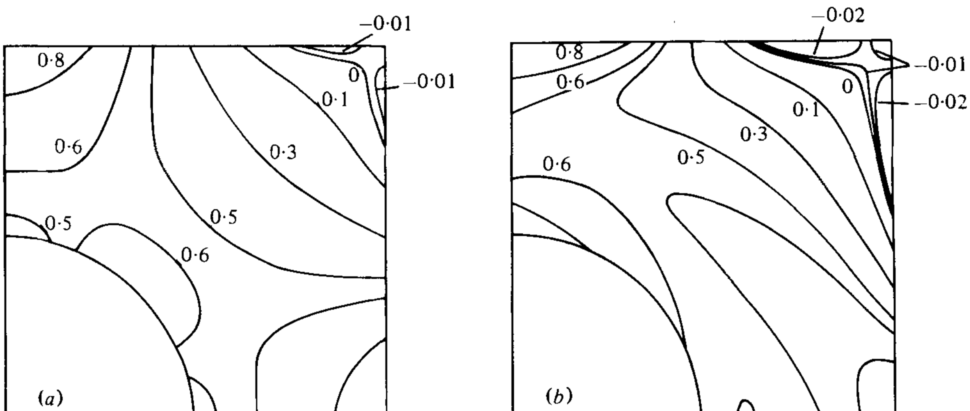

FIGURE 9 (a), (b). For legend see p. 511.

of separation and attachment. Furthermore, the intensity of the corner eddy falls considerably, as shown in figure 10, and this behaviour is in direct contrast to that for $B = 2$.

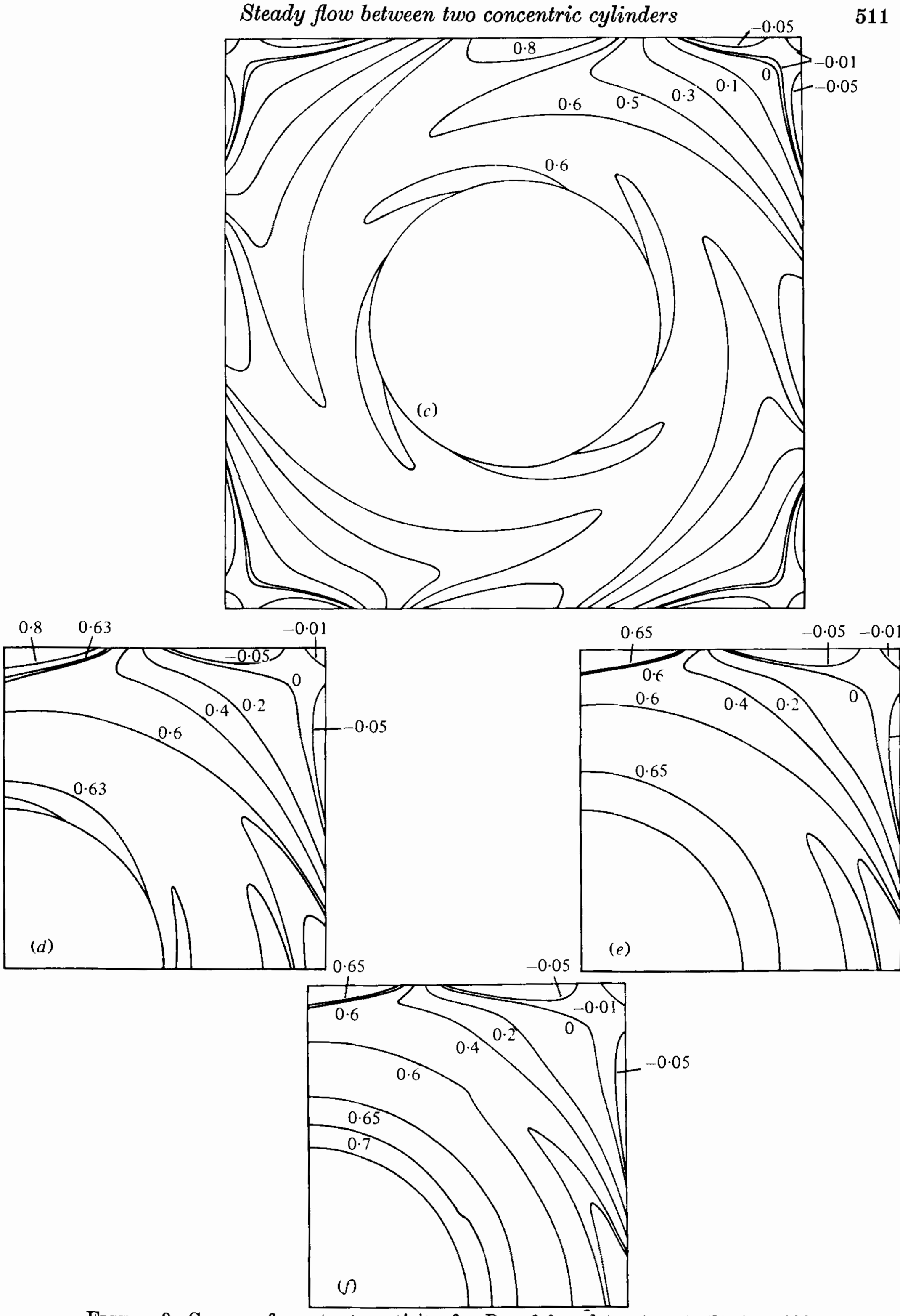

FIGURE 9. Curves of constant vorticity for $B = 2{\cdot}0$ and (a) $R = 1$, (b) $R = 100$, (c) $R = 200$, (d) $R = 500$, (e) $R = 1000$, (f) $R = 1400$.

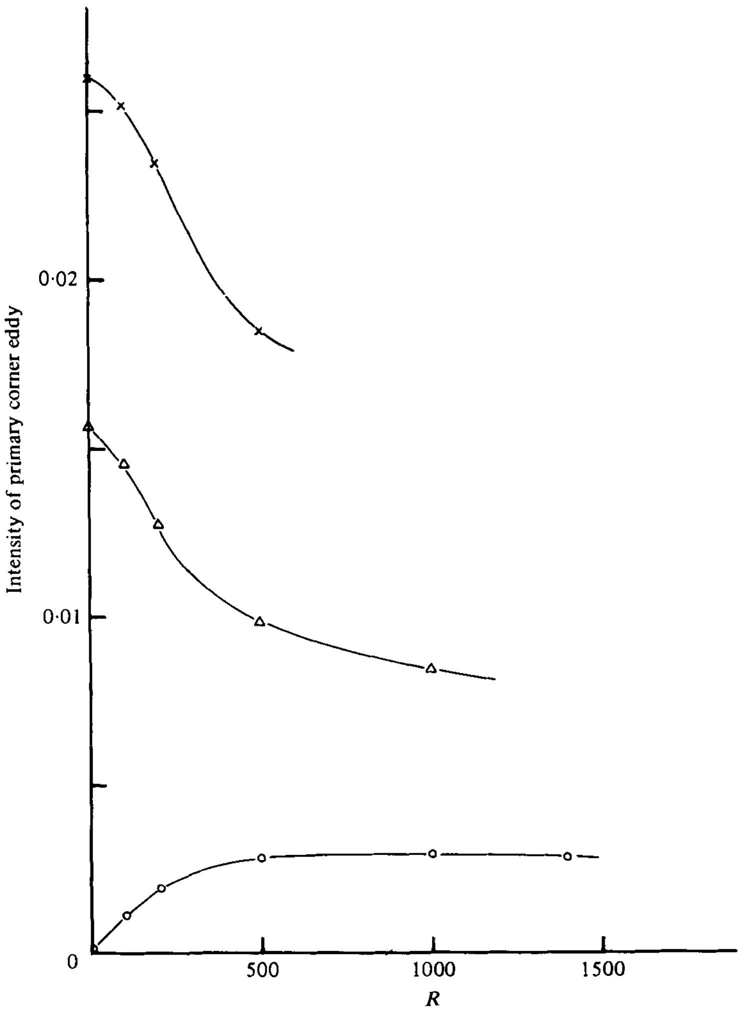

FIGURE 10. Variation of the intensity of the primary eddy with R: $\times$, $B = 1{\cdot}05$; $\triangle$, $B = 1{\cdot}1$; $\bigcirc$, $B = 2{\cdot}0$.

The variation of the vorticity curves with increasing R is not as marked as in the case of $R = 2$ though the curves still become distorted in the direction of rotation. The magnitude of the vorticity is considerably greater for both $B = 1{\cdot}05$ and $1{\cdot}1$ than it is for $B = 2$, the maximum vorticity being about 39·0 and 19·0 respectively compared with about 1·3 for $B = 2$.

In the corner region, Moffatt (1964) has shown that a sequence of eddies dying away into the corner exists and this behaviour has been verified numerically by Pan & Acrivos (1967) and Collins & Dennis (1976). In the present investigation the second eddy is just discernible but this and further eddies could have been exhibited more clearly by using the mesh refinement technique of Collins & Dennis.

The author wishes to thank Professor M. H. Rogers for originally suggesting the problem and for his helpful discussions.

REFERENCES

BATCHELOR, G. K. 1956 *J. Fluid Mech.* **1**, 177.
BATCHELOR, G. K. 1967 *An Introduction to Fluid Dynamics*. Cambridge University Press.
BURGGRAF, O. R. 1966 *J. Fluid Mech.* **24**, 113.
COLLINS, W. M. & DENNIS, S. C. R. 1975 *Quart. J. Mech. Appl. Math.* **28**, 133.
COLLINS, W. M. & DENNIS, S. C. R. 1976 *J. Fluid Mech.* **76**, 417.
GREENSPAN, D. 1969 *Comp. J.* **12**, 89.
GREENSPAN, D. 1973 *J. Fluid Mech.* **57**, 167.
KAWAGUTI, M. 1961 *J. Phys. Soc. Japan* **16**, 2307.
MEYER, K. A. 1969 *Phys. Fluids Suppl.* **12**, II 165.
MOFFATT, H. K. 1964 *J. Fluid Mech.* **18**, 1.
PAN, F. & ACRIVOS, A. 1967 *J. Fluid Mech.* **28**, 643.
ROACHE, P. J. 1976 *Computational Fluid Dynamics*. Hermosa Publishers.
ROGERS, E. M. & BEARD, D. W. 1969 *J. Comp. Phys.* **4**, 1.